Sensitivity of Streamflow Characteristics to Different Spatial Land-Use Configurations in Tropical Catchment

Hero Marhaento[1]; Martijn J. Booij[2]; T. H. M. Rientjes[3]; and Arjen Y. Hoekstra[4]

Abstract: This paper analyzed the impact of land use and its spatial configuration on streamflow in the Samin catchment (278 km^2), Indonesia. Historic land use was reconstructed based on satellite images for the years 1982, 1994, 2000, 2006, and 2013. A calibrated and validated Soil and Water Assessment Tool (SWAT) simulated the catchment hydrology of the study area, taking respective land use covers as inputs. A correlation analysis between changes in land use covers and simulated streamflow characteristics was carried out. A land-cover scenario analysis assessed the sensitivity of streamflow characteristics to different future land use covers. The results show that an increase in the settlement connectivity can result in an increase in the ratio of surface runoff to streamflow and a decrease in the ratio of dry-season streamflow to wet-season streamflow, and vice versa. The results suggest that land use pattern management can be an important component in water management. **DOI:** 10.1061/(ASCE)WR.1943-5452.0001122. *© 2019 American Society of Civil Engineers.*

Author keywords: Catchment hydrology; Land use change; Deforestation; Runoff characteristics; Soil and water assessment tool (SWAT) model.

Introduction

In the last decades, the role of land use and impacts of land use changes on catchment hydrology have received much attention. Numerous studies argue that different types of land use have different water-use and water-storage characteristics, and thus different land uses and their spatial distributions may result in different distributions of water in space and time (Wigmosta and Burges 1990; Sahin and Hall 1996; Bruijnzeel 1989, 2004; Brown et al. 2005; Romanowicz and Booij 2011; Gumindoga et al. 2014a; Zhang et al. 2016; Marhaento et al. 2017b). Studies in tropical regions have shown that land use changes from vegetated areas into settlements may significantly reduce canopy interception and soil infiltration capacity, resulting in a larger fraction of rainfall being transformed into surface runoff (Bruijnzeel 2004; Valentin et al. 2008; Marhaento et al. 2017b). In addition, the spatial distribution of land uses may affect the hydrological response of catchments; for example, the volume and peak flow discharges of surface runoff entering a stream may change (Su et al. 2014; Wheater and Evans 2009). Carter et al. (2005) considered land use policy to be a relevant factor with reference to increased demands for settlement and agricultural land by rapid population growth. Wheater and Evans (2009) and Zhang et al. (2013) indicated that land-use management can be used as a measure in water management practice for flood prevention and drought mitigation.

Increases in settlements and farming areas can be in discordance with the availability of water resources. For instance, settlement development can lead to a reduction in soil infiltration rates and consequently an increase of surface runoff and a decrease in dry-weather base flow (Bruijnzeel 2004; Marhaento et al. 2017a, b). Agricultural intensification could lead to changes in infiltration and actual evapotranspiration and thus affect dry-weather base flow (Bruijnzeel 1989; Brown et al. 2005). Therefore, future land allocation and land-use management should be designed based on an understanding of how land-use changes may affect catchment hydrology (e.g., Carter et al. 2005).

Most studies assessing the effects of land-use change on hydrological processes and behavior have focused on the impact of changes in the relative presence of different land-use types. Less attention has been given to the impacts of changes in spatial land-use configurations (e.g., shape and connectivity of land-use types). The impact of the spatial land-use configuration on water resources, however, is relevant when selecting a particular land-use management strategy (Azevedo et al. 2005; O'Connell et al. 2007; Bakker et al. 2008; Ding et al. 2016; Roberts 2016; Boongaling et al. 2018). Relevant concerns include, for example, the effect of choosing specific locations for certain new land uses (e.g., high versus low elevations), and the effect of different spatial configurations (e.g., small-scattered versus large-clustered) of forest planting and harvesting strategies. A better understanding will give insight into the potential effects of alternative land-use allocations and thus configurations on water availability at the catchment scale (Lin et al. 2007; Boongaling et al. 2018). Fig. 1 depicts different spatial land-use configurations which may result in different hydrological responses.

The impact of land use on hydrological processes is often studied by means of a paired catchment approach, in which land use in the control catchment is held constant while land use in the treatment catchment, having similar physical conditions, is changed. Measurements then focus on the differences in hydrological response

[1]Researcher, Faculty of Forestry, Universitas Gadjah Mada, Yogyakarta 55281, Indonesia; Water Engineering and Management Group, Faculty of Engineering Technology, Univ. of Twente, 7522 NB Enschede, Netherlands (corresponding author). ORCID: https://orcid.org/0000-0001-5601-6261. Email: marhaento@ugm.ac.id

[2]Associate Professor, Water Engineering and Management Group, Faculty of Engineering Technology, Univ. of Twente, 7522 NB Enschede, Netherlands. ORCID: https://orcid.org/0000-0001-6208-9045

[3]Associate Professor, Dept. of Water Resources, Faculty of Geo-Information Science and Earth Observation, Univ. of Twente, 7514 AE Enschede, Netherlands.

[4]Professor, Water Engineering and Management Group, Faculty of Engineering Technology, Univ. of Twente, 7522 NB Enschede, Netherlands; Institute of Water Policy, Lee Kuan Yew School of Public Policy, National Univ. of Singapore, Singapore 259770, Singapore.

Note. This manuscript was submitted on April 30, 2018; approved on March 22, 2019; published online on September 25, 2019. Discussion period open until February 25, 2020; separate discussions must be submitted for individual papers. This paper is part of the ***Journal of Water Resources Planning and Management***, © ASCE, ISSN 0733-9496.

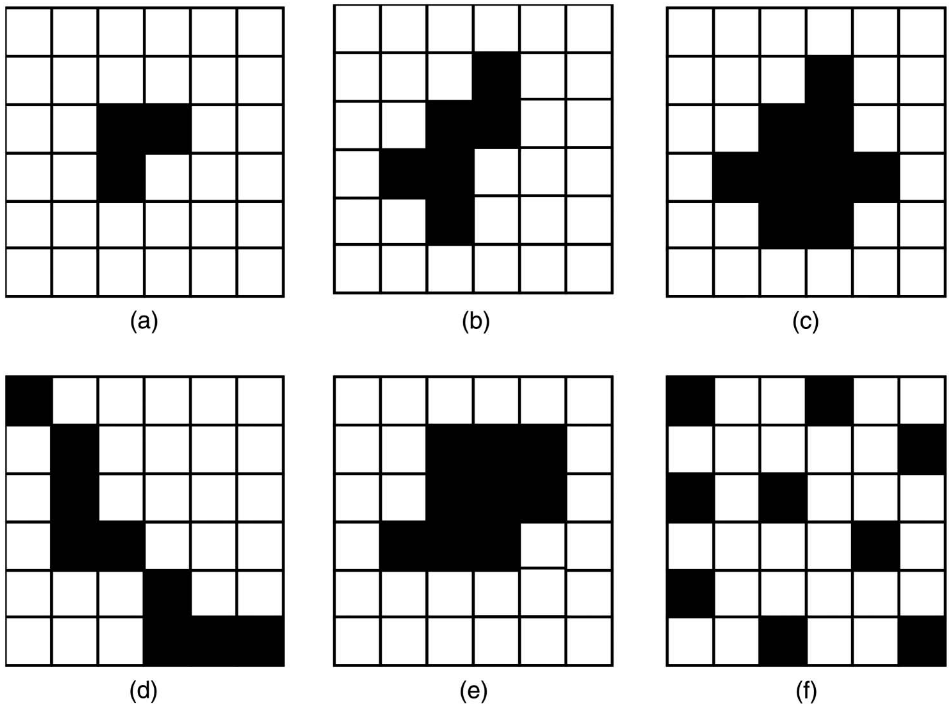

Fig. 1. Six grids of 6×6 cells showing differences in percentage of a certain land-use type (e.g., settlements) and differences in spatial configuration of this land-use type in the landscape. Grids (a–c) show an increase in percentage, from 8.3% to 16.7% to 25% of the total area, respectively. Grids (d–f) show changes in the spatial configuration (e.g., shape and connectivity) with the percentage of the land-use type maintained at 25% of the total area.

between the control and treatment catchment (Fohrer et al. 2005). Suryatmojo et al. (2011) used this approach to assess the impacts of different forest harvesting strategies (i.e., selective logging) on the streamflow characteristics in Central Kalimantan, Indonesia, and found that applications of different forest harvesting strategies resulted in different hydrological responses (i.e., peak flows). Sahin and Husesall (1996) and Brown et al. (2005) reviewed the results of numerous paired catchment studies worldwide and found that changes in land use through deforestation, afforestation, regrowth, and forest conversion can affect annual streamflow, which is likely to increase with the percentage of forest removed. Although a paired catchment study can provide relevant information of changes in hydrological processes due to changes in land use, this method mostly is applicable to small catchments (<25 km^2), for which uncertainties due to spatial heterogeneity are relatively small (Fohrer et al. 2005; Brown et al. 2005).

For larger catchments (>100 km^2), a modeling approach is typically used. Zhang et al. (2013) generated various hypothetical land-use configurations using a land-use change model and used these as input for a grid-based hydrological model to assess the impacts of land-use configurations on streamflow in the Yong Ding catchment (300 km^2), China. They found that land-use fragmentation may affect streamflow characteristics at different spatial resolutions. At fine scale (30×30 m^2), increases in fragmented grassland have resulted in increases in peak flow and total streamflow, whereas at coarse scale ($1{,}200 \times 1{,}200$ m^2), forest fragmentation has resulted in increases in peak flow and total streamflow. Li and Zhou (2015) assessed the correlation between various land-use configuration characteristics and hydrological variables (i.e., streamflow and sediment yield) in the Yanhe catchment (7,725 km^2), China, and found that changes in the land-use configurations significantly changed the sediment yield but did not significantly change the streamflow. Bormann et al. (2009) used different hydrological models [i.e.,water balance simulation model (WASIM), TOPMODEL-based land surface-atmosphere transfer scheme (TOPLATS), and soil and water assessment tool (SWAT)] to assess the sensitivity of water balance components to different land-use configurations in the Dill catchment (693 km^2), Germany. In their method, land use was redistributed in different ways (e.g., randomly distributed land use and land-use distribution based on topography), whereas the areal fractions of the land-use classes were maintained. They found that redistributing land use slightly affected the water balance components. These studies show that the relationships between land-use configurations and hydrological processes atthe catchment scale are not fully understood and require further study.

This paper assesses the impacts of land-use configurations on streamflow characteristics of the Samin catchment (278 km^2) in Java, Indonesia. The semidistributed physically based Soil and Water Assessment Tool model (Arnold et al. 1998) was used to simulate hydrological processes of the study catchment. In the first part of this study, land-use maps over the period 1982–2013 were reconstructed by means of LANDSAT images from the years 1982, 1994, 2000, 2006, and 2013. Fifteen landscape metrics were calculated using FRAGSTATS version 4.2 (McGarigal and Marks 1995) to define spatial land-use pattern characteristics for each year. These selected metrics represent a wide range of land-use pattern characteristics and were previously reported to have a relationship with hydrological processes (Lin et al. 2007; Zhang et al. 2013; Li and Zhou 2015). In the second part of this study, correlations between land-use metrics and annual streamflow characteristics simulated by the SWAT model were determined. Streamflow characteristics considered were the ratio of simulated surface runoff to streamflow (Q_s/Q), and the ratio of dry-season streamflow and wet-season streamflow (Q_{dry}/Q_{wet}). Estimates of Q_s, Q, Q_{dry} and Q_{wet} are at an annual scale for different land-use configurations and result from a calibrated SWAT model at daily time step (Marhaento et al. 2017b); Q_s/Q and Q_{dry}/Q_{wet} were selected for analysis following the results of Zhang et al. (2013) who argued that these were mostly affected by changes in the land-use configuration. In addition, Q_s/Q is often used at an annual scale as an indicator of the ratio of quick catchment responses to catchment streamflow (Suryatmojo et al. 2011), whereas Q_{dry}/Q_{wet} can be used as a measure to show the seasonal distribution of water availability within the catchment (Romanowicz and Booij 2011). For the third part of this study, two hypothetical land-use scenarios were developed in order to assess the sensitivity of streamflow characteristics to different spatial land-use configurations. In this scenario analysis, land-use planning for the study catchment available from the Central Java Provincial Government (2010) was used as a baseline scenario, and its spatial configuration was changed while maintaining the percentage of each land-use type. Finally, the potential hydrological impacts as simulated by the SWAT model for different land-use configurations in the study catchment were assessed. Because land-use planning was used to develop land-use scenarios, the results of these scenario analysis can support the exploration of potential hydrological impacts of alternative land-use configurations. In addition, the results of this study can be useful for authorities to mitigate the main problems in watershed management, such as soil erosion and seasonally unbalanced water availability (i.e., droughts in the dry season and floods in the wet season). We describe the study area and data used in section "Study Area and Data Availability." Section "Method" covers the methods used in this study. Section "Results" presents the results, section "Discussion" discusses the key findings, and section "Conclusions" draws the conclusions from this study.

Study Area and Data Availability

Catchment Description

The Samin river is a tributary of the Bengawan Solo river, the longest river in Java, Indonesia. The source of the river is the Lawu Mountain [3,175 m above sea level (a.s.l.)]. The Samin catchment area is about 278 km^2, situated between 7.6° and 7.7° south latitude and 110.8° and 111.2° east longitude. The mean elevation of the catchment is 380 m, the mean slope 19.8%, and the stream density around 2.2 km/km^2. The soil composition of the Samin catchment is predominantly Luvisols, a leafy humus soil that can be mainly found in the midstream and downstream areas, and Andosols, a volcanic soil that can be mainly found in the upstream area near the Lawu Mountain. These soils cover 57% and 43% of the study area, respectively. The Samin catchment has a tropical monsoon climate with a distinct wet season (November–April) and dry season (May–October), with January–March being the wettest period and July–September the driest period of the year. In the period 1990–2013, the mean daily temperature varied between 21.5°C and 30.5°C, the annual rainfall varied between 1,500 and 3,000 mm, the annual potential evapotranspiration varied between 1,400 and 1,700 mm, and the annual streamflow varied between 500 and 1,200 mm (Marhaento et al. 2017a). Fig. 2 shows the Samin catchment with its topography and the location of hydrometeorological gauges. A water level gauge is located at the outlet and recorded daily water level data for the period 1990–2013. Eleven precipitation stations recorded daily precipitation and three meteorological stations recorded daily maximum and minimum temperature, relative humidity, wind speed, and solar radiation for the same period as the water level data. All the hydrological data were provided by the Bengawan Solo River Basin office.

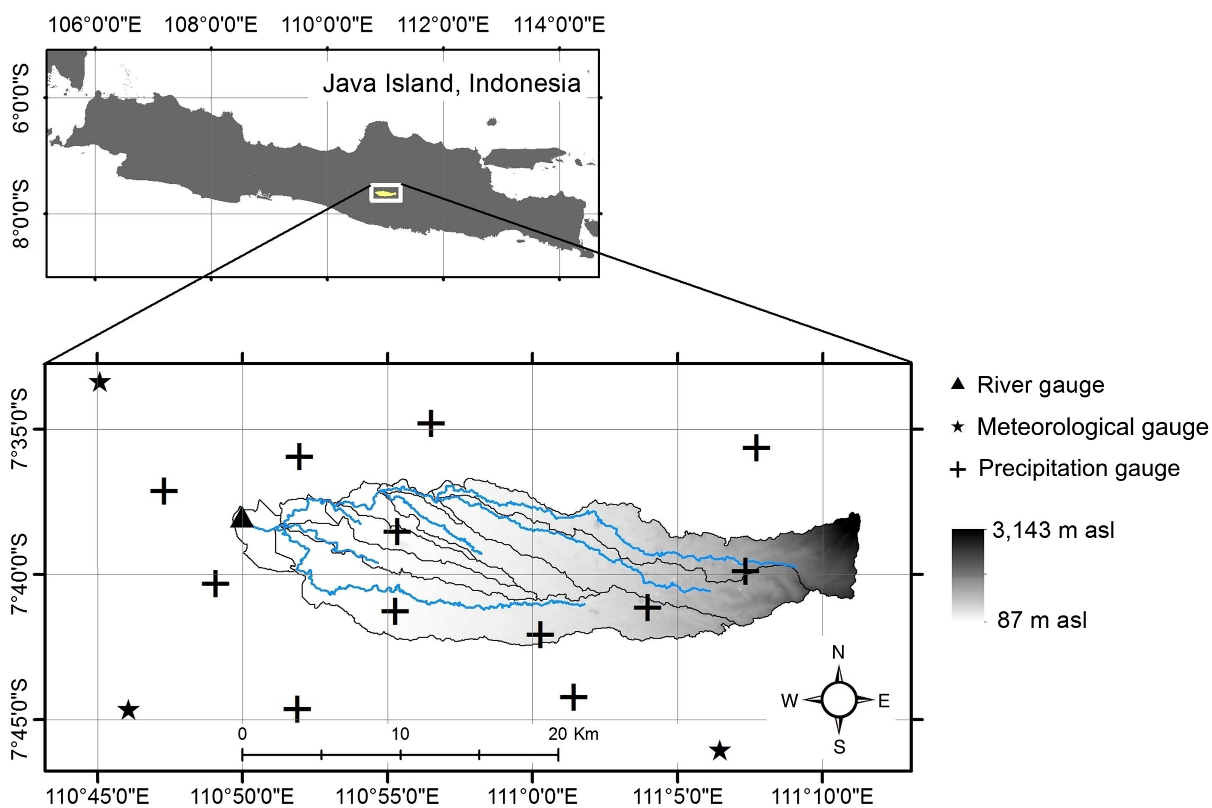

Fig. 2. Location of the Samin catchment in Java, Indonesia, with locations of hydrometeorological gauges provided by the Bengawan Solo River Basin office.

Data Availability

Various data sets are available for modelling hydrological processes of the study catchment, such as a digital elevation model (DEM), land-use data, soil data, and climate data. The DEM was generated from a contour map with a contour interval of 12.5 m, which was made available by the Indonesia Geospatial Information Agency. Furthermore, the DEM was used to delineate the catchment and subcatchment boundaries and to generate a slope map. Land-use maps with a spatial resolution of 30 m for the years 1994, 2000, 2006, and 2013 were available for the study area from Marhaento et al. (2017b). An additional land-use image for September 11, 1982 was acquired from the LANDSAT satellite (USGS 2017) to represent land use for the year 1982. A soil map at 30-arc s spatial resolution was available from the Harmonized World Soil Database (FAO et al. 2012). A land-use spatial planning map of the study area for the period 2009–2029 was available with a spatial scale of 1:500.000 from the Central Java Provincial Government (2010). Daily climate data were available from eleven rainfall stations and three meteorological stations (Fig. 2) for the period 1983–2013, provided by the Bengawan Solo River Basin office and the Adi Sumarmo Airport. The Bengawan Solo River Basin office provided daily water level data in the Samin catchment for the period 1990–2013, including the rating curve to convert the water level data into discharge data for model calibration. We used the same climate and discharge data set as Marhaento et al. (2017a), who filled and corrected time series of the daily climatological and discharge data of the Samin catchment.

Method

Reconstruction of Land Use, 1982–2013

Land use in the study area over the period 1982–2013 was reconstructed based on LANDSAT images from the years 1982, 1994, 2000, 2006, and 2013, following the approach of Marhaento et al. (2017b). Image processing analysis was carried out only for 1982 because the land-use maps of the other years were available from Marhaento et al. (2017b). The LANDSAT images for 1982 were processed through two steps: preprocessing and image classification. Preprocessing included a nonsystematic geometric correction to avoid distortion of map coordinates and a masking analysis to remove the area outside the study area. Image classification was performed using a maximum-likelihood approach based on 1,000 ground-control points (GCPs) that were generated from an institutional land-use map (scale 1:25,000) from the Geospatial Information Agency of Indonesia, in which half of the sample points were used to perform accuracy assessment using an error matrix (Congalton 1991). Two accuracy assessment measures were used, namely the overall accuracy and the Kappa coefficient. The overall accuracy is the total number of correct samples divided by the total number of samples. The Kappa coefficient is the coefficient of agreement between the classification map and the reference data. The results of the accuracy assessment showed that the average overall accuracy and Kappa coefficient of land-use maps used for this study were 89% and 87%, respectively, which is sufficient for producing a land-use map (Congalton 1991).

For this study, land-use classes from Marhaento et al. (2017b) were reclassified into four land-use classes: forest area (combining evergreen forest and mixed garden), agricultural area (combining paddy field and dry land farming), settlements, and other areas (combining shrub, bare land, and water body). The latter covers less than 5% of the catchment area.

In order to characterize land-use configurations for respective years, landscape metrics for each land-use type were calculated using FRAGSTATS (McGarigal et al. 2012). Landscape metrics are quantitative indexes that describe spatial aspects (e.g., size and edge, shape, and connectivity) of landscapes based on spatial data (Kupfer 2012). FRAGSTATS software can be used to calculate numerous landscape metrics simultaneously within a GIS. It has been widely used in landscape analysis including its relations with hydrological processes (Lin et al. 2007; Zhang et al. 2013; Li and Zhou 2015).

Landscapes can be analyzed at different spatial levels, namely cell, patch, class, and landscape levels. The selection of the appropriate level for analysis depends on the level of heterogeneity for the question under consideration (McGarigal et al. 2012). This study focused on the class level because we analyzed aspects of configuration for individual land-use types within a catchment. Because numerous landscape metrics are available with redundant information, only 15 metrics that relate to land-use characteristics and that have a relation to hydrological processes (Lin et al. 2007; Zhang et al. 2013; Li and Zhou 2015) were selected. These metrics include five metrics that describe landscape size and edge, namely percentage of land-use type (PL), number of patches (NP), patch density (PD), largest patch index (LPI), and edge density (ED); five metrics that describe landscape shape (i.e., geometric complexity of patch types), namely perimeter:area ratio (PAR), shape index (SHI), fractal dimension index (FDI), related circumscribing circle (RCC), and contiguity index (CI); and five metrics that describe landscape aggregation (i.e., tendency of patch types to be spatially aggregated), namely Euclidian nearest neighborhood distance (ENN), proportion of like adjacencies (PLA), splitting index (SPI), landscape shape index (LSI), and patch cohesion index (PCI). Table 1 briefly describes these landscape metrics. A detailed description of the landscape metrics, including their equations, was given by McGarigal and Marks (1995).

Hydrological Model Simulations

Hydrological processes were simulated using the SWAT model (Arnold et al. 1998), a physically based semidistributed hydrological model operating at a daily time step, which has proven its suitability for hydrologic impact studies around the world (Wagner et al. 2013; Memarian et al. 2014; Brauman et al. 2015; Marhaento et al. 2017b). The SWAT model divides a catchment into subcatchments and further divides each subcatchment into hydrological response units (HRUs), at which level a land-phase water balance is calculated (Neitsch et al. 2011). A HRU is defined as a lumped area within a catchment assumed to have uniform hydrological behavior and is characterized by a dominant land-use type, soil type, and slope (Arnold et al. 1998). A daily water balance is computed for each HRU for each subcatchment, and runoff is routed through channels to the catchment outlet, where the water balance of the catchment is calculated in depth units (millimeters). A SWAT model calibrated and validated for the Samin catchment was available from a previous study (Marhaento et al. 2017b). In the current study, equal SWAT model settings were applied as in the previous study. Here, we briefly summarize the model setup and parameterizations; a detailed description was given by Marhaento et al. (2017b).

Eleven subcatchments ranging in size from 0.12 to 83 km^2 were generated from the DEM. A land-use map with four classes (i.e., forest, settlement, agriculture, and other areas), a slope map with five classes (i.e., 0%–8%, 8%–15%, 15%–25%, 25%–45%, and >45%), and a soil map with three classes (i.e., Luvisols, Andosols, and Vertisols) were used to create hydrological response units by spatially overlying maps of land-use, soil, and slope classes.

J. Water Resour. Plann. Manage., 2019, 145(12): 04019054

Table 1. Descriptions of landscape metrics used in this study

Landscape metric (abbreviation)	Description
Percentage of land-use type (PL)	PL quantifies the proportional abundance of area of each land-use type in the landscape. PL = 100 when there is only one land-use type in the landscape.
Number of patches (NP)	NP quantifies the number of patches of the corresponding land-use type in the landscape. NP = 1 if the land use consists of a single patch.
Patch density (PD)	PD quantifies the ratio of number of patches of each land-use type over the landscape area. PD value increases when land use becomes more fragmented.
Largest patch index (LPI)	LPI quantifies the percentage of landscape comprised by the largest patch. LPI = 100 when the landscape consists of a single patch of the corresponding land-use type.
Edge density (ED)	ED quantifies the ratio of edge segment length to total area. ED value increases when the patch shapes become more irregular due to longer edge between patch types.
Perimeter:area ratio (PAR)	PAR quantifies the ratio of the patch perimeter (meters) to area (square meters). PAR value increases without limit depending on the patch shape.
Shape index (SHI)	SHI quantifies the complexity of the patch shape within each class relative to a square shape. SHI = 1 when all patches of land-use type are square (grid).
Fractal dimension index (FDI)	FDI quantifies the shape complexity across a range of spatial scales (patch sizes). FDI value approaches 1 for shapes with (very) simple perimeters such as squares.
Related circumscribing circle (RCC)	RCC quantifies the ratio between patch sizes to the smallest circumscribing circle area. RCC = 0 for circular patches and approaches 1 for elongated, linear patches one cell wide.
Contiguity index (CI)	CI quantifies the spatial connectedness, or contiguity, of cells within a grid-cell patch to provide an index of patch boundary configuration. CI = 0 for a one-pixel patch and increases to a limit of 1 as patch contiguity increases.
Euclidian nearest neighborhood distance (ENN)	ENN quantifies the shortest straight-line distance between the focal patch and its nearest neighbor of the same land-use class. ENN approaches 0 as the distance to the nearest neighbor decreases.
Proportion of like adjacencies (PLA)	PLA quantifies the degree of aggregation of the focal patch type that is shown by the frequency of different pairs of patch types appear side-by-side on the map. PLA = 0 when the corresponding patch type is maximally disaggregated and there are no like adjacencies.
Splitting index (SPI)	SPI quantifies the number of patches with a constant patch size when the landscape is subdivided into S patches, where S is the value of the splitting index. SPI = 1 when the landscape consists of single patch and it increases as the landscape is increasingly subdivided into smaller patches.
Landscape shape index (LSI)	LSI quantifies the class aggregation within the landscape, and equals 1 when the landscape consists of a single square or maximally compact (i.e., almost square) patch of the corresponding type.
Patch cohesion index (PCI)	PCI quantifies the physical connectedness of the corresponding patch type. PCI value ranges from 0 to 100, and increases as the patch type is more clumped in its distribution, And hence more physically connected.

Source: Adapted from McGarigal and Marks (1995).

For land use, this study used a coarser land-use classification than Marhaento et al. (2017b), and thus crop parameters for each land-use class used in this study are averages because different land use and vegetation covers fall within a single HRU. The crop parameter for forest is the average value of evergreen forest (FRSE) and mixed garden (FRST) parameters. The crop parameter for agriculture is the average value of dryland farming (AGRR) and paddy field (RICE) parameters. For the settlement, the class Urban Residential Medium Density (URMD) in SWAT was used to assign parameters of the settlement area. URMD assumes an average of 38% impervious area in the settlement area (Neitsch et al. 2011), which is relatively similar to the settlement conditions in the study catchment.

The Penman–Monteith method and the Soil Conservation Service Curve Number (SCS CN) method were used to calculate reference evapotranspiration and surface runoff, respectively. For flow routing, we used the Muskingum method, which models the storage volume as a combination of wedge and prism storages (Neitsch et al. 2011). Six SWAT parameters, namely CN2, SOL_AWC, ESCO, CANMX, GW_DELAY, and GW_REVAP, were identified as the most sensitive parameters following the procedure from Abbaspour et al. (2015). These parameters were calibrated based on the observed discharge using the Latin hypercube sampling approach from the Sequential Uncertainty Fitting version 2 (SUFI-2) in the SWAT-Calibration and Uncertainty Procedure (SWAT-CUP) package on a monthly basis. The calibration period was 1990–1995 and the validation period was 1996–2013. The initial parameter ranges were determined based on minimum and maximum values allowed in SWAT. A number of iterations were performed, in which each iteration consisted of 1,000 simulations with narrowed parameter ranges in subsequent calibration rounds. Simulations for model calibration were assessed on a monthly basis and the Nash–Sutcliffe efficiency (NSE) was used as the objective function. In addition to the NSE, other model performance statistics, including percent bias (PBIAS), the squared correlation coefficient (R^2), RMSE, and the mean absolute error (MAE), were calculated to evaluate the performance of the hydrological models. The results of the model calibration showed that the simulated mean monthly discharge in the calibration period agreed well with the observed records, with NSE, PBIAS, R^2, RMSE and MAE values of 0.78, −7.8, 0.78, 3.6, and 2.7 m^3/s, respectively. In the validation period (1996–2013), the NSE value was 0.70 and values for the other metrics, namely PBIAS, R^2, RMSE and MAE, were 0.6, 0.76, 3.4, and 2.5 m^3/s, respectively.

Changes in Land-Use and Streamflow Characteristics

Effects of past land-use changes on hydrological processes were simulated using the calibrated SWAT model, using as inputs land-use cover in the years 1982, 1994, 2000, 2006, and 2013 and observed meteorological time series in the period 1983–2013, with a 2-year warming-up period. Each land-use cover was simulated separately with the same meteorological input so that the differences obtained from the simulations were due only to the differences in land use. For each simulation, the ratio of mean annual surface runoff to streamflow (Q_s/Q) and the ratio of dry-season streamflow to wet-season streamflow (Q_{dry}/Q_{wet}) was determined. All water balance components were simulated by the SWAT model at the catchment level in millimeters and therefore can be directly used to calculate the water balance ratios.

J. Water Resour. Plann. Manage., 2019, 145(12): 04019054

From the mean monthly rainfall from 1983–2013, July–September (JAS) is the driest period of the year and January–March (JFM) is the wettest. For this reason, we accumulated streamflow in the periods JAS and JFM to represent streamflow in the dry season and the wet season, respectively. Furthermore, the relationships between changes in land-use metrics and streamflow characteristics were analyzed using Pearson's correlation statistic. Two hypotheses were tested at a significance level of 1%, namely a null hypothesis assuming no correlation between changes in land-use metrics and streamflow characteristics, and an alternative hypothesis for which there is a correlation between changes in land-use metrics and streamflow characteristics. We carried out the correlation analysis at a significance level of 1% due to the small size of the samples ($n = 5$).

Simulation of Land-Use Scenarios

In order to explore changes in streamflow characteristics in relation to changes in land-use patterns, we simulated hydrological processes under different land-use scenarios. In this scenario analysis, we changed the spatial configuration of the land-use planning of the study area available from the Central Java Provincial Government (2010), whereas the percentages of different land-use types were fixed (Fig. 1). The land-use planning was used as a baseline scenario and provides spatial constraints for the land-use scenarios. We selected land-use planning because it is assumed to be the future direction of land-use management in the study area. Developing land-use scenarios based on the land-use planning can support the exploration of potential hydrological impacts of alternative land-use planning. Land-use scenarios were developed at a $250 \times 250\ m^2$ spatial resolution following the spatial scale of the land-use planning.

According to the land-use planning, settlements are located in the elevation range from 0 to 1,000 m a.s.l. and slope range from 0% to 15%, agriculture is located in the elevation range from 0 to 1,000 m a.s.l and slope range from 0% to 20%, and forest is located in the elevation range from 100 to 3,125 m a.s.l. and slope range from 0% to 50%. Based on these spatial constraints, locations above 1,000 m a.s.l. and slope >20% are allocated only to forest area, whereas other locations can be for every land-use type, thus giving room to develop land-use configuration scenarios. Within these constraints, two opposite land-use scenarios were created to represent a wide range of possible configurations. In the clustered land-use scenario we combined each land-use type at the subcatchment level following the guideline from the Presidential Regulation of the Republic of Indonesia No. 32 (1990), in which settlements are grouped and positioned at low elevations and on flat to middle slopes, agriculture is grouped and positioned at middle elevations and on flat to middle slopes, and forest is grouped and positioned at high elevations and on steep slopes. In the scattered land-use scenario we split each land-use class at the subcatchment level into several patches and spread them within the catchment. In the land-use redistribution process, we maintained the mean elevation and slope of each land-use class so that land-use classes in this scenario have a similar mean elevation and slope as in the land-use planning.

Results

Land Use, 1982–2013

Fig. 3 shows the land-use configurations in the Samin catchment for different years in the period 1982–2013. Changes in land use over this period can be characterized by a significant decrease in forest area (−36.1%), which mainly were converted into settlement area (+29.6%) and agriculture area (+7.7%), whereas changes in other land-use types were relatively small (−1.2%). The forest area decreased by 4.2% over the period 1982–1994, by 6.6% over 1994–2000, by 16.1% over 2000–2006 and by 9.2% over 2006–2013, whereas the settlement area increased by 5%, 6.5%, 9.4%, and 8.7% over the four respective periods. Agriculture area increased by 1.5% in the period 1982–1994, then decreased by 2.4% in the period 1994–2000, and increased again by 8.6% in the period 2000–2013. The decrease of agriculture area in the period 1994–2000 was due to a massive land-use conversion from agriculture area to housing and public facilities (e.g., roads, buildings) as a result of the population boom in the 1990s (Verburg and Bouma 1999).

Changes in the distribution of land-use types in the period 1982–2013 were accompanied by changes in spatial land-use patterns. Table 2 lists the landscape metric values for 1982, 1994, 2000, 2006, and 2013 per land-use type. The decrease in the percentage of forest was associated with a decrease in the largest patch index and the patch cohesion index, whereas there was no clear relation with other metrics. LPI quantifies the percentage of the landscape composed by the largest patch, whereas PCI quantifies the physical connectivity of patches from the corresponding land-use type. The LPI value for forest was 41.5 in 1982, but decreased to 38.2 (1994), 17.2 (2000), 5.1 (2006), and 2.3 (2013), whereas the PCI value for forest was 99.8 in 1982, and decreased to 99.7 (1994), 99.2 (2000), 98.2 (2006), and 97 (2013). The increase in the percentage of settlement area was associated with an increase in the edge density and the PCI values, whereas there was no clear relation with other metrics. ED quantifies the ratio of edge segment length to total area. The ED value for settlement was 10.8 in 1982 and increased to 24.3 (1994), 39.9 (2000), 41.9 (2006), and 53.9 (2013), whereas the PCI value of settlement was 91.1 in 1982 and increased to 91.3 (1994), 92.5 (2000), 96.2 (2006), and 98.8 (2013). For agriculture, this study found no relations between changes in the percentage of land use and changes in the other metrics.

Correlations between Land-Use Patterns and Streamflow Characteristics

Land-use changes in the period 1982–2013 have affected streamflow characteristics as simulated by the SWAT model (Fig. 4). The ratio of mean annual surface runoff to streamflow (Q_s/Q) increased from 0.28 in 1982 to 0.31 (1994), 0.33 (2000), 0.36 (2006), and 0.39 (2013), whereas the ratio of dry-season to wet-season streamflow ($Q_{\mathrm{dry}}/Q_{\mathrm{wet}}$) decreased from 0.13 in 1982 to 0.12 (1994), 0.11 (2000), 0.1 (2006), and 0.09 (2013). A consistent increase of Q_s/Q and a consistent decrease of $Q_{\mathrm{dry}}/Q_{\mathrm{wet}}$ is in line with the direction of changes in forest and settlement area, because forest significantly decreased and settlement significantly increased in the period 1982–2013.

Based on the results of Pearson's correlation analysis between various landscape metrics and streamflow characteristics, it was found that only four metrics, namely the percentage of forest (PL_f), the percentage of settlement (PL_s), the cohesion of forest area (PCI_f), and the cohesion of settlement (PCI_s), were significantly correlated (i.e., the alternative hypothesis is accepted) with Q_s/Q at a significance level of 1%; PL_f and PCI_f had a negative correlation with Q_s/Q, whereas PL_s and PCI_s had a positive correlation with Q_s/Q. For $Q_{\mathrm{dry}}/Q_{\mathrm{wet}}$, it was found that only three metrics, namely the percentage of forest, the percentage of settlement, and the cohesion of settlement, were significantly correlated at a significance level of 1%; PL_f had a positive correlation with $Q_{\mathrm{dry}}/Q_{\mathrm{wet}}$, whereas the percentage of settlement and the cohesion

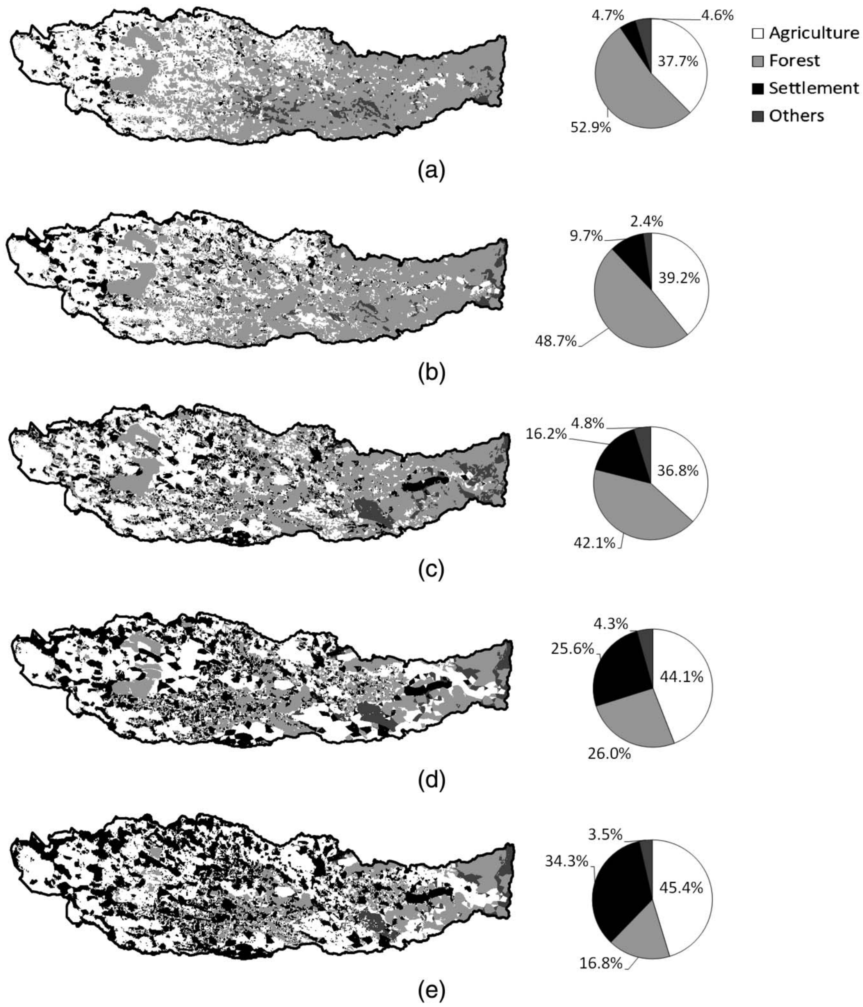

Fig. 3. Land-use distribution of the Samin catchment in (a) 1982; (b) 1994; (c) 2000; (d) 2006; and (e) 2013.

Table 2. Landscape metrics for 1982, 1994, 2000, 2006, and 2013 for agriculture, settlement, and forest

Year	Metrics														
	PL	NP	PD	LPI	ED	PAR	SHI	FDI	RCC	CI	ENN	PLA	SPI	LSI	PCI
Agriculture															
1982	37.8	390	1.4	28.9	49.1	508	1.5	1.1	0.6	0.6	140	90.2	12	33.3	99.7
1994	39.2	764	2.7	27.6	60.1	639	1.4	1	0.5	0.5	104	88.5	13	39.9	99.6
2000	36.9	791	2.8	13.5	55.8	635	1.4	1.1	0.5	0.5	102	88.7	36	38.3	99.1
2006	44.3	702	2.5	19.6	49.9	599	1.3	1	0.5	0.5	106	91.5	23	31.2	99.2
2013	45.5	690	2.5	31.7	60.5	609	1.4	1	0.5	0.5	99	90	10	37.3	99.6
Settlement															
1982	4.7	262	0.9	0.3	10.8	438	1.4	1.1	0.6	0.6	247	82.8	24,185	20.6	91.1
1994	9.7	856	3.1	0.9	24.3	604	1.2	1	0.5	0.5	140	81.2	6,409	32.5	91.3
2000	16.1	997	3.6	0.8	39.9	611	1.4	1.1	0.5	0.5	108	81.4	3,933	41.4	92.5
2006	25.4	629	2.3	1.4	41.9	462	1.4	1.1	0.5	0.6	110	87.6	837	34.6	96.2
2013	34.2	821	3	10.4	53.9	536	1.3	1	0.5	0.5	110	88.2	76	38.4	98.8
Forest															
1982	52.9	655	2.4	41.5	52	580	1.3	1	0.5	0.5	118	92.6	6	29.8	99.8
1994	48.7	720	2.6	38.2	55.7	579	1.3	1	0.5	0.5	124	91.4	7	33.2	99.7
2000	42.2	698	2.5	17.2	62.4	497	1.5	1.1	0.5	0.6	110	88.9	24	40	99.2
2006	25.9	661	2.4	5.1	36.8	553	1.3	1	0.5	0.5	132	89.4	167	30.1	98.2
2013	16.8	711	2.6	2.3	29.4	623	1.3	1	0.5	0.5	145	86.9	545	29.9	97

Note: PL = percentage of land-use type (%); NP = number of patches; PD = patch density (number/100 ha); LPI = largest patch index (%); ED = edge density (m/ha); PAR = perimeter:area ratio; SHI = shape index; FDI = fractal dimension index; RCC = related circumscribing circle; CI = contiguity index; ENN = Euclidian nearest neighborhood distance (m); PLA = proportion of like adjacencies (%); SPI = splitting index; LSI = landscape shape index; and PCI = patch cohesion index.

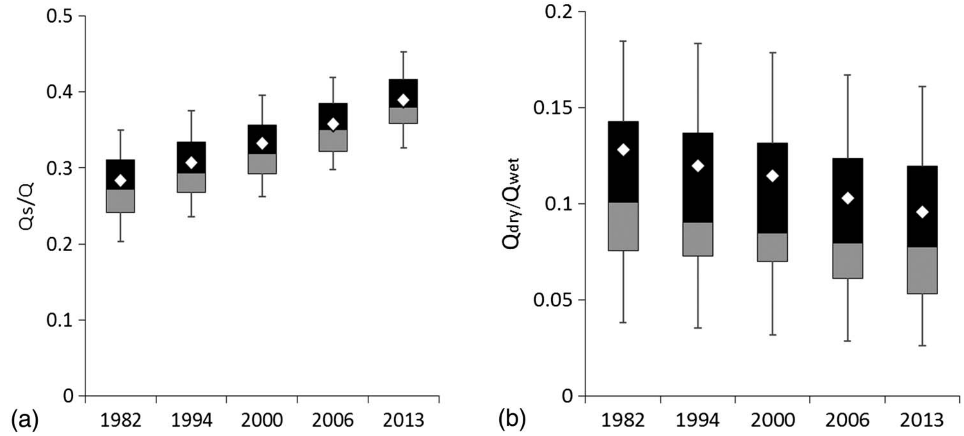

Fig. 4. (a) Box-whisker plot of the ratio of mean annual surface runoff to streamflow (Q_s/Q); and (b) box-whisker plot of the ratio of mean annual streamflow in the dry season to streamflow in the wet season ($Q_{\mathrm{dry}}/Q_{\mathrm{wet}}$) from simulations using land-use cover from different years. White diamonds represent mean values.

of settlement had a negative correlation with $Q_{\mathrm{dry}}/Q_{\mathrm{wet}}$. Fig. 5 shows the estimated Pearson's correlation coefficients between landscape metrics and streamflow characteristics.

Changes in Streamflow Characteristics under Different Land Configuration Scenarios

The correlation analysis shows that the percentages of forest and settlement and the patch cohesion index of forest and settlement were the metrics that best correlated with streamflow characteristics ($\alpha = 1\%$). It was expected that PL_s and PL_f, would significantly affect streamflow characteristics based on previous studies for the Samin catchment (Marhaento et al. 2017a, b). An increase in PL_s and at the same time a decrease in PL_f increased mean annual streamflow (Q). In addition, the fraction of streamflow originating from surface runoff significantly increased, compensated by a decrease in base flow. This led to an increase in the ratio of mean annual surface runoff to streamflow (Q_s/Q) and at the same time a decrease in the ratio of dry-season streamflow to wet-season streamflow ($Q_{\mathrm{dry}}/Q_{\mathrm{wet}}$).

The relations of PCI_s and PCI_f, with the streamflow characteristics independent of the percentage of settlement and forest area was assessed using the scenario analysis. Fig. 6 shows the land-use distribution of the baseline scenario (i.e., land-use planning), the clustered land-use scenario, and the scattered land-use scenario, and Fig. 7 shows the differences of PCI values for each land-use scenario compared with the baseline scenario. The clustered scenario had larger PCI values and the scattered scenario had smaller PCI values than the baseline scenario.

At the catchment scale, the results of the simulations show that the clustered and scattered scenarios reduced the long-term average of Q_s/Q. Compared with the baseline scenario, the long-term ratio of Q_s/Q decreased from 0.37 to 0.35 under the clustered scenario and from 0.37 to 0.36 under the scattered land-use scenario. The long-term ratio of $Q_{\mathrm{dry}}/Q_{\mathrm{wet}}$ increased under the clustered land-use scenario and decreased under the scattered scenario. Simulations using different land configuration scenarios may result in different hydrological responses (Fig. 8). However, the changes in the long-term ratios of Q_s/Q and $Q_{\mathrm{dry}}/Q_{\mathrm{wet}}$ at the catchment scale under different scenarios were relatively small (i.e., from -0.02 to $+0.01$).

The effect of changes in the patch connectivity on the streamflow characteristics can be better observed at the subcatchment level, in particular for changes in PCI_s; Q_s/Q increased to $+0.1$ following an increase in PCI_s by as much as $+0.9$, with a coefficient of determination (R^2) of about 0.5 under the clustered scenario, whereas Q_s/Q decreased by as much as -0.2 following a decrease in PCI_s by as much as -2.4, with a R^2 of about 0.6 under the scattered scenario (Fig. 9). Conversely, $Q_{\mathrm{dry}}/Q_{\mathrm{wet}}$ increased by as much as $+0.02$ following a decrease in the PCI_s by as much as -2.4 with a R^2 of about 0.7 under the scattered scenario, whereas less clear impacts on $Q_{\mathrm{dry}}/Q_{\mathrm{wet}}$ under the clustered scenario occurred (i.e., $R^2 = 0.3$). Whereas the effects of changes in PCI_s on the streamflow characteristics were discernible, there was no clear relation between PCI_f and the streamflow characteristics, for which R^2 was less than 0.2 under both clustered and scattered scenarios.

Discussion

The study shows that changes in the streamflow characteristics of the study catchment can be attributed to both changes in the percentages of the land-use types and changes in the physical connectivity between patches of similar land-use types. We found that the decrease of vegetation and the increase of impervious areas were likely the cause of substantial changes in simulated streamflow by the SWAT model. A consistent decline of forest area in the catchment due to conversion into settlement area resulted in a larger volume of rainfall transformed into surface runoff. With less water infiltrated into and stored in the soil, an increased fraction of rainfall will become surface runoff and a less balanced water distribution between the wet and dry seasons can be expected. Our findings regarding the relationship between changes in the percentages of different land-use types and changes in the streamflow characteristics confirm those of earlier studies (e.g., Bruijnzeel 1989, 2004; Badhuri et al. 2001; Brown et al. 2005; Wagner et al. 2013; Remondi et al. 2016; Gumindoga et al. 2014b; Marhaento et al. 2017a, b).

When the percentages of different land-use types are fixed but the configuration and physical connectivity of patches is changed, changes in streamflow characteristics occur at both the catchment and subcatchment levels. We found that changes at the catchment level (278 km^2) were very small and not consistent (e.g., the long-term ratio of surface runoff to streamflow decreased for both clustered and scattered scenarios at the catchment scale, whereas the long-term ratio of dry-season streamflow to wet-season streamflow responded differently under scattered and clustered scenarios). Apparently, the different patch cohesion indexes from different land-use scenarios only slightly affect the streamflow characteristics. A clearer relationship between streamflow characteristics and patch

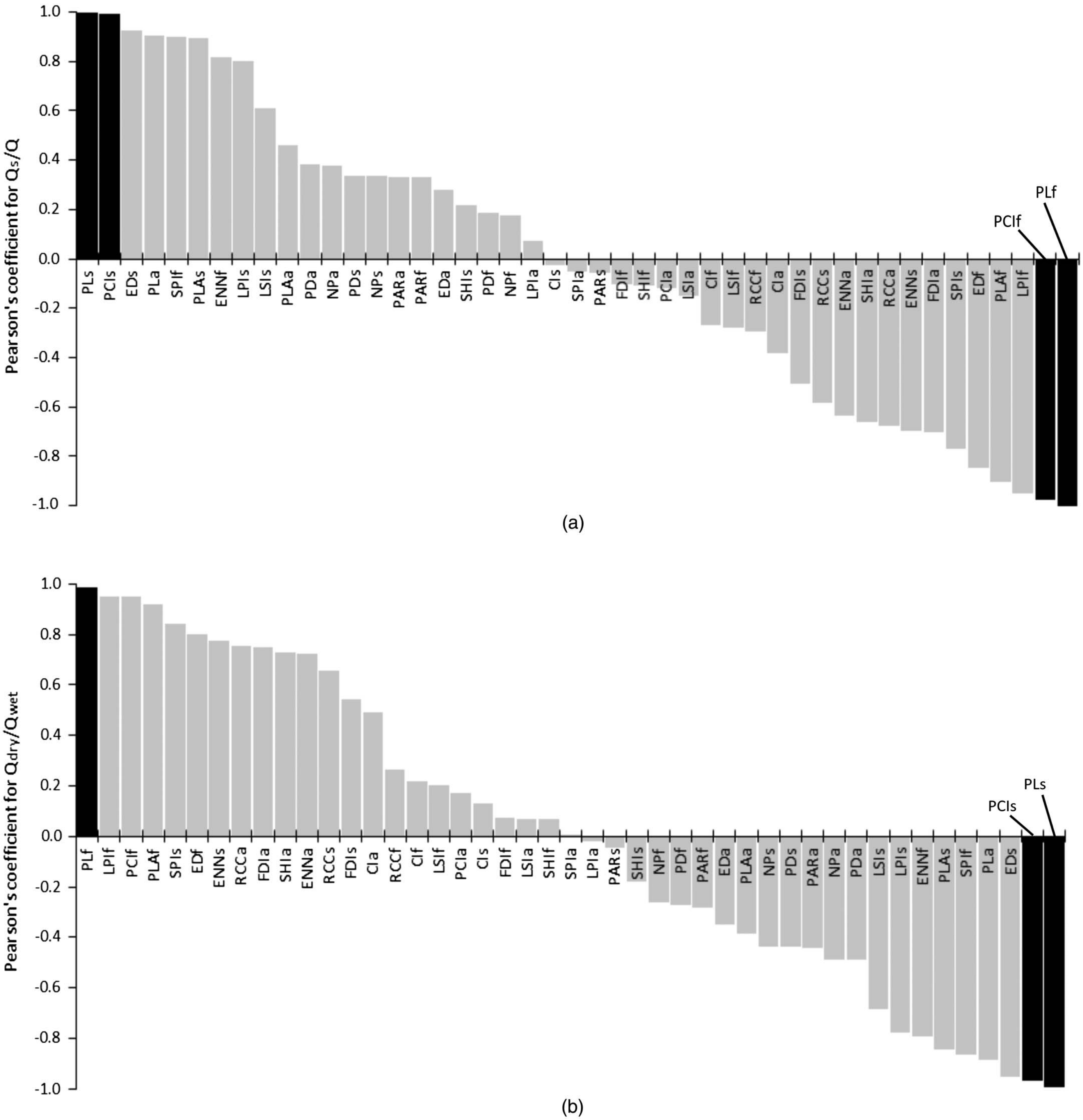

Fig. 5. (a) Pearson's correlation coefficient for relations between landscape metrics and the ratio of mean annual surface runoff to streamflow (Q_s/Q); and (b) ratio of dry-season streamflow to wet-season streamflow ($Q_{\rm dry}/Q_{\rm wet}$). Solid bars show landscape metrics with a significance level of 1%; a, f, and s denote agriculture, forest, and settlement, respectively.

connectivity occurred at the subcatchment scale (0.12–83 km^2), where Q_s/Q was positively correlated and $Q_{\rm dry}/Q_{\rm wet}$ was negatively correlated with increases in patch connectivity of settlements. Apparently, the opposite impacts of changes in the patch connectivity at the subcatchment scale compensated each other at the catchment level. We expected that the clustered forest area in the upstream part would reduce Q_s/Q and increase $Q_{\rm dry}/Q_{\rm wet}$, whereas the clustered settlement area in the downstream part would increase Q_s/Q and decrease $Q_{\rm dry}/Q_{\rm wet}$. With different directions of changes in streamflow characteristics between upstream and downstream areas within the catchment, long-term changes of those variables at the catchment level canceled each other out. This is similar to the findings by Wagner et al. (2013) and Wilk and Hughes (2002), who argued that the net hydrological result at the catchment level can mask the impacts of land-use changes on hydrological processes at the subcatchment scale.

The impacts of changes in the patch connectivity of settlement on streamflow characteristics were more pronounced than the

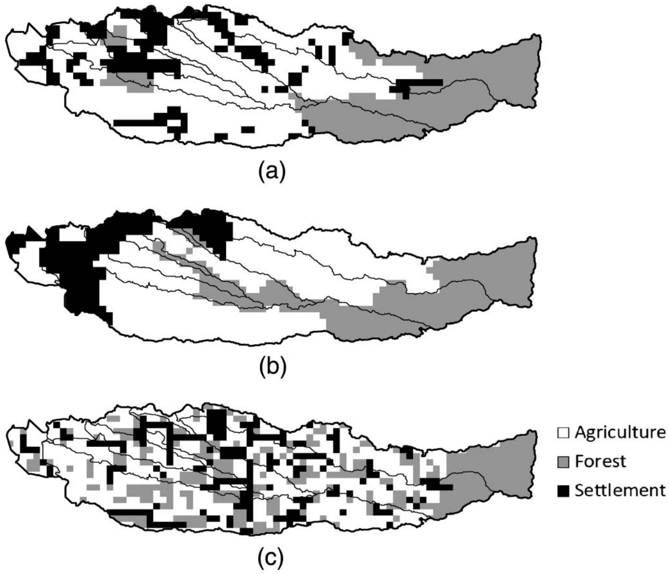

Fig. 6. Land-use configuration of (a) baseline scenario (i.e., land-use planning); (b) clustered scenario; and (c) scattered scenario. Land-use scenarios represent different cohesion values (PCI), whereas percentages of different land-use types (PL) are fixed.

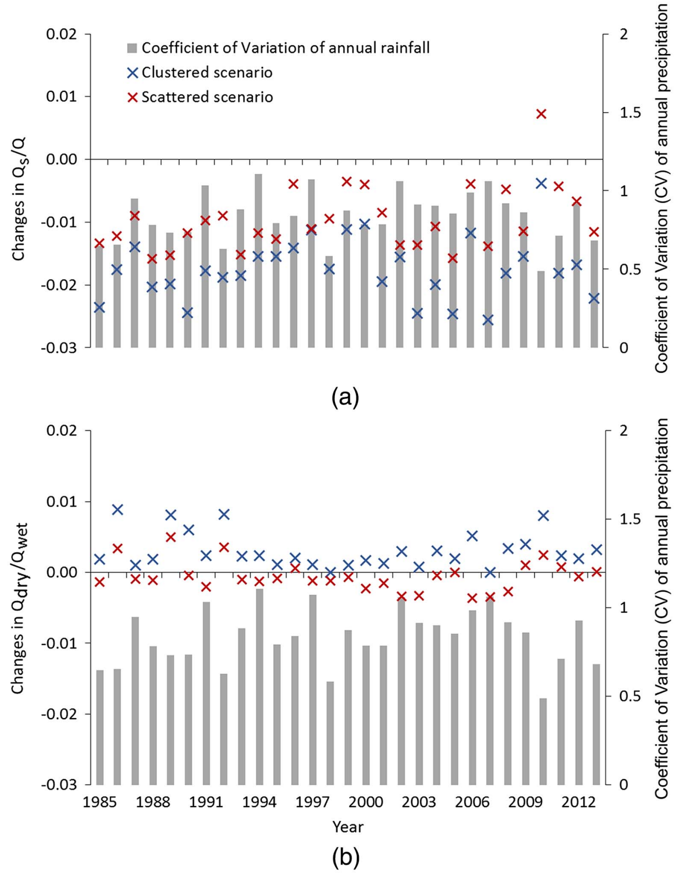

Fig. 8. Changes in metrics under different scenarios relative to the baseline scenario, including coefficient of variation of annual precipitation for the period 1985–2013: (a) ratio of surface runoff to total runoff (Q_s/Q); and (b) ratio of streamflow in the dry season to streamflow in the wet season ($Q_{\text{dry}}/Q_{\text{wet}}$).

impacts of changes in the patch connectivity of forest. We agree with Mejía and Moglen (2009), Wagner et al. (2013), and Su et al. (2014), who argued that urban imperviousness patterns within catchments can play an important role in determining changes in streamflow characteristics, particularly because of changes in the fraction of flow becoming surface runoff. When the settlement area is clustered, peak flows will increase without much affecting the flow volume compared with scattered settlement (Corbett et al. 1997). When the urban development is located in the downstream area near the catchment outlet (as simulated in this study under the clustered scenario), more-pronounced impacts can be expected compared with settlement scattered over the catchment (Su et al. 2014; Wheater and Evans 2009).

We found that the percentages of different land-use types strongly affect the runoff generation of the study catchment, whereas the patch connectivity for a certain land-use type may affect surface runoff and the seasonal balance of flows by accelerating or decelerating runoff responses. However, the spatial heterogeneity of hydrological response over catchments is scale-dependent, and the landscape metrics may change with changing scale (McGarigal and Marks 1995; McGarigal et al. 2012) as well as dominant hydrological processes (Blöschl et al. 2007; Zhang et al. 2013). This study used a semidistributed SWAT model that simulates hydrological processes in each

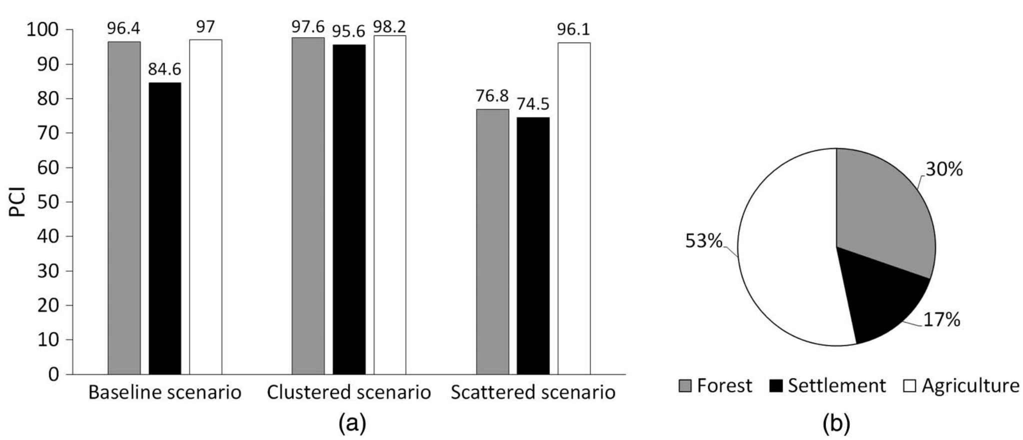

Fig. 7. (a) Patch cohesion index (PCI) of each land use type for different land use scenarios; and (b) percentages of the different land use types (PL).

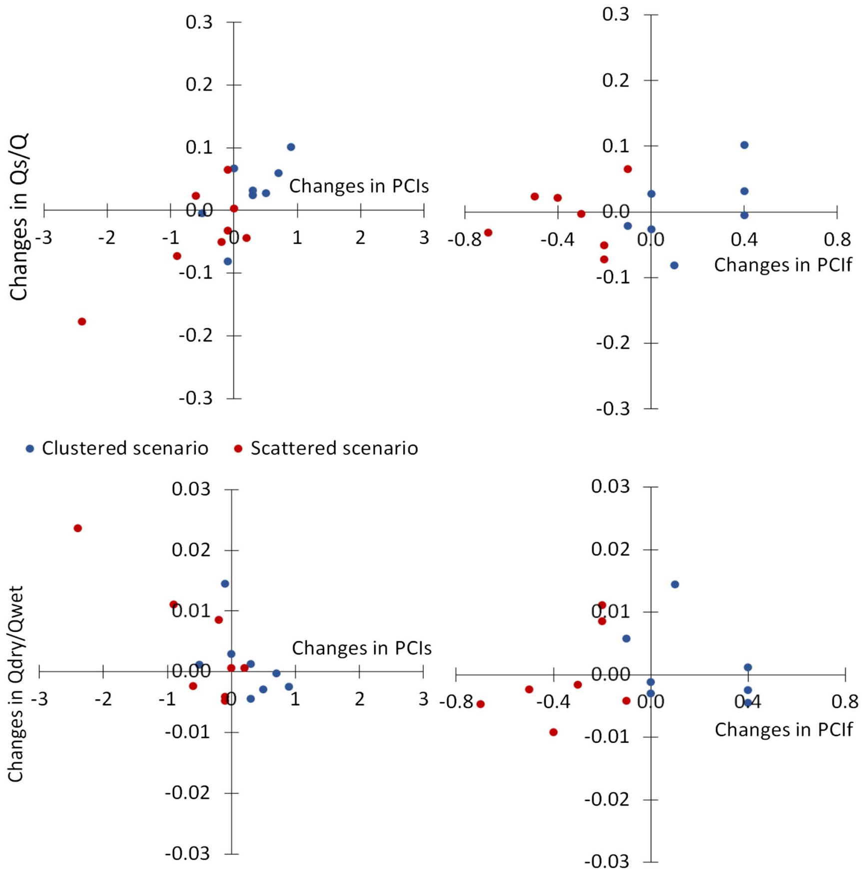

Fig. 9. Relationship between changes in the patch cohesion index for settlement (PCI_s) and forest (PCI_f) and changes in streamflow characteristics relative to the baseline scenario.

Hydrological Response Unit within subcatchments. Thus, the water balance simulation is at the HRU level, which is a combination of land-use type, soil type, and slope class. With the coarse scale of land-use scenarios used in this study, we might have lost spatial detail of changes in the land-use configurations. Both land-use scenarios provided relatively small changes in the patch connectivity at the subcatchment scale (Fig. 9). Although the results show relatively clear signals for changes in the streamflow characteristics due to changes in the patch connectivity, a more discernible signal can be expected if the land-use change scenarios are developed at a finer scale. The SWAT model is able to simulate streamflow only at the subcatchment level, so the spatial flow variation between HRUs within a subcatchment is not taken into account. With this model limitation, changes in hydrological processes due to changes in land-use patterns cannot be presented at a smaller scale than the subcatchment scale. To further investigate the impacts of different land-use metrics on streamflow characteristics, we suggest using a fully distributed model, e.g., the Gridded Surface Subsurface Hydrologic Analysis (GSSHA) model (Zhang et al. 2013) and the Regional Hydro-Ecological Simulation System (RHESSys) model (Tague and Band 2004).

Although the effects of climate variability were isolated in the simulations by forcing the model with the same meteorological input for different land-use inputs, the contribution of climate variability to changes in streamflow characteristics cannot be neglected. The hydrological response to different land-use scenarios varied across years, likely due to rainfall variability (Fig. 8). Marhaento et al. (2018) found for the same study area that changes in the rainfall variability may have large impacts on the water availability of the study catchment.

Findings of this study offer an opportunity to include hydrological impact considerations in developing land-use plans. For the study catchment, the existing land-use planning is projected to reduce the mean annual streamflow and surface runoff, and increase the mean annual base flow and evapotranspiration (Marhaento et al. 2018). By altering the spatial patterns of the land-use plan, e.g., by scattering settlement area in the downstream area and clustering forest area in the upstream area, surface runoff can be reduced and a more balanced distribution of streamflow between the dry season and the wet season can be achieved. Because land-use planning always occurs at different spatial scales (e.g., national, provincial, and district scales), multiscale analysis of the impacts of land-use patterns on streamflow characteristics is recommended.

Conclusions

This study assessed the effects of changes in land-use patterns on streamflow characteristics in the Samin catchment and found that changes in the ratio of surface runoff to streamflow (Q_s/Q) and the ratio of dry-season streamflow to wet-season streamflow ($Q_{\mathrm{dry}}/Q_{\mathrm{wet}}$) are significantly affected by the percentage of forest and settlement (PL_f and PL_s) and the patch cohesion index of forest and settlement (PCI_f and PCI_s). Simulations with the SWAT model indicated that a decrease of PL_f and PCI_f and an increase of PL_s and PCI_s cause an increase of Q_s/Q and a decrease of $Q_{\mathrm{dry}}/Q_{\mathrm{wet}}$. Individually, changes in PCI may affect the streamflow characteristics; clear relationships were found at the subcatchment level. Simulating the impact of two hypothetical land-use scenarios, a clustered scenario and a scattered scenario, found that an increase in PCI_s with PL_s maintained constant may result in an increase of Q_s/Q and a decrease of Q_{dry}/Q_{wet}, and vice versa, whereas changes in PCI_f with PL_f maintained constant have less impact on streamflow characteristics. The findings show that, particularly for settlements, altering the spatial configuration can be an effective measure to achieve a more favorable distribution of streamflow between the dry season and the wet season.

Acknowledgments

The authors acknowledge the Bengawan Solo River Basin Organization, Ministry of Public Works, Indonesia and the Bengawan Solo Watershed Research Centre, Ministry of Environment and Forestry, Indonesia for providing the hydrological and climatological data. The first author expresses his appreciation to the Directorate General of Higher Education, Ministry of Research, Technology and Higher Education of the Republic of Indonesia, for the financial support during his Ph.D. project.

References

Abbaspour, K. C., E. Rouholahnejad, S. Vaghefi, R. Srinivasan, H. Yang, and B. Kløve. 2015. "A continental-scale hydrology and water quality model for Europe: Calibration and uncertainty of a high-resolution large-scale SWAT model." *J. Hydrol.* 524 (May): 733–752. https://doi.org/10.1016/j.jhydrol.2015.03.027.

Arnold, J. G., R. Srinivasan, R. S. Muttiah, and J. R. Williams. 1998. "Large area hydrologic modeling and assessment. Part I: Model development." *J. Am. Water Resour. Assoc.* 34 (1): 73–89. https://doi.org/10.1111/j.1752-1688.1998.tb05961.x.

Azevedo, J. C., J. R. Williams, M. G. Messina, and R. F. Fisher. 2005. "Impacts of the sustainable forestry initiative landscape level measures on hydrological processes." *Water Resour. Manage.* 19 (2): 95–110. https://doi.org/10.1007/s11269-005-1503-5.

Bakker, M. M., G. Govers, A. van Doorn, F. Quetier, D. Chouvardas, and M. Rounsevell. 2008. "The response of soil erosion and sediment export to land-use change in four areas of Europe: The importance of landscape pattern." *Geomorphology* 98 (3): 213–226. https://doi.org/10.1016/j.geomorph.2006.12.027.

Bhaduri, B., M. Minner, S. Tatalovich, and J. Harbor. 2001. "Long-term hydrologic impact of urbanization: A tale of two models." *J. Water Resour. Plann. Manage.* 127 (1): 13–19. https://doi.org/10.1061/(ASCE)0733-9496(2001)127:1(13).

Blöschl, G., S. Ardoin-Bardin, M. Bonell, M. Dorninger, D. Goodrich, D. Gutknecht, D. Matamoros, B. Merz, P. Shand, and J. Szolgay. 2007. "At what scales do climate variability and land cover change impact on flooding and low flows?" *Hydrol. Processes* 21 (9): 1241–1247. https://doi.org/10.1002/hyp.6669.

Boongaling, C. G. K., D. V. Faustino-Eslava, and F. P. Lansigan. 2018. "Modeling land use change impacts on hydrology and the use of landscape metrics as tools for watershed management: The case of an ungauged catchment in the Philippines." *Land Use Policy* 72 (Mar): 116–128. https://doi.org/10.1016/j.landusepol.2017.12.042.

Bormann, H., L. Breuer, T. Gräff, J. A. Huisman, and B. Croke. 2009. "Assessing the impact of land use change on hydrology by ensemble modelling (LUCHEM) IV: Model sensitivity to data aggregation and spatial (re-)distribution." *Adv. Water Resour.* 32 (2): 171–192. https://doi.org/10.1016/j.advwatres.2008.01.002.

Brauman, K. A., D. L. Freyberg, and G. C. Daily. 2015. "Impacts of land-use change on groundwater supply: Ecosystem services assessment in Kona, Hawaii." *J. Water Resour. Plann. Manage.* 141 (12): A4014001. https://doi.org/10.1061/(ASCE)WR.1943-5452.0000495.

Brown, A. E., L. Zhang, T. A. McMahon, A. W. Western, and R. A. Vertessy. 2005. "A review of paired catchment studies for determining changes in water yield resulting from alterations in vegetation." *J. Hydrol.* 310 (1–4): 28–61. https://doi.org/10.1016/j.jhydrol.2004.12.010.

Bruijnzeel, L. A. 1989. "(De)Forestation and dry season flow in the tropics: A closer look." *J. Trop. For. Sci.* 1 (3): 229–243.

Bruijnzeel, L. A. 2004. "Hydrological functions of tropical forests: Not seeing the soil for the trees?" *Agric., Ecosyst. Environ.* 104 (1): 185–228. https://doi.org/10.1016/j.agee.2004.01.015.

Carter, N., R. D. Kreutzwiser, and R. C. de Loë. 2005. "Closing the circle: Linking land use planning and water management at the local level." *Land Use Policy* 22 (2): 115–127. https://doi.org/10.1016/j.landusepol.2004.01.004.

Central Java Provincial Government. 2010. "The regional regulation of Central Java province number 6 (year 2010): Spatial planning of Central Java province 2009–2029." Accessed May 14, 2017. http://ditjenpp.kemenkumham.go.id/files/ld/2010/ProvinsiJawaTengah-2010-6.pdf.

Congalton, R. G. 2011. "A review of assessing the accuracy of classifications of remotely sensed data." *Remote Sens. Environ.* 37 (1): 35–46. https://doi.org/10.1016/0034-4257(91)90048-B.

Corbett, C. W., M. Wahl, D. E. Porter, D. Edwards, and C. Moise. 1997. "Nonpoint source runoff modeling A comparison of a forested watershed and an urban watershed on the South Carolina coast." *J. Exp. Mar. Biol. Ecol.* 213 (1): 133–149. https://doi.org/10.1016/S0022-0981(97)00013-0.

Ding, J., Y. Jiang, Q. Liu, Z. Hou, J. Liao, L. Fu, and Q. Peng. 2016. "Influences of the land use pattern on water quality in low-order streams of the Dongjiang River basin, China: A multi-scale analysis." *Sci. Total Environ.* 551–552 (May): 205–216. https://doi.org/10.1016/j.scitotenv.2016.01.162.

FAO, IIASA, ISRIC, ISSCAS, and JRC (Food and Agriculture Organization of the United Nations, International Institute for Applied Systems Analysis, International Soil Reference and Information Centre, Institute of Soil Science – Chinese Academy of Sciences, and Joint Research Centre of the European Commission). 2012. *Harmonized world soil database (version 1.2)*. Rome: FAO.

Fohrer, N., S. Haverkamp, and H. G. Frede. 2005. "Assessment of the effects of land use patterns on hydrologic landscape functions: Development of sustainable land use concepts for low mountain range areas." *Hydrol. Processes* 19 (3): 659–672. https://doi.org/10.1002/hyp.5623.

Gumindoga, W., T. Rientjes, M. D. Shekede, D. T. Rwasoka, I. Nhapi, and A. T. Haile. 2014a. "Hydrological impacts of urbanization of two catchments in Harare, Zimbabwe." *Remote Sens.* 6 (12): 12544–12574. https://doi.org/10.3390/rs61212544.

Gumindoga, W., T. H. M. Rientjes, A. T. Haile, and T. Dube. 2014b. "Predicting streamflow for land cover changes in the Upper Gilgel Abay River Basin, Ethiopia: A TOPMODEL based approach." *Phys. Chem. Earth, Parts A/B/C* 76–78: 3–15. https://doi.org/10.1016/j.pce.2014.11.012.

Kupfer, J. A. 2012. "Landscape ecology and biogeography: Rethinking landscape metrics in a post-FRAGSTATS landscape." *Prog. Phys. Geogr.* 36 (3): 400–420. https://doi.org/10.1177/0309133312439594.

Li, J., and Z. X. Zhou. 2015. "Coupled analysis on landscape pattern and hydrological processes in Yanhe watershed of China." *Sci. Total Environ.* 505 (Feb): 927–938. https://doi.org/10.1016/j.scitotenv.2014.10.068.

Lin, Y. P., N. M. Hong, P. J. Wu, C. F. Wu, and P. H. Verburg. 2007. "Impacts of land use change scenarios on hydrology and land use patterns in the Wu-Tu watershed in Northern Taiwan." *Landscape Urban Plann.* 80 (1): 111–126. https://doi.org/10.1016/j.landurbplan.2006.06.007.

Marhaento, H., M. J. Booij, and A. Y. Hoekstra. 2017a. "Attribution of changes in stream flow to land use change and climate change in a mesoscale tropical catchment in Java, Indonesia." *Hydrol. Res.* 48 (4): 1143–1155. https://doi.org/10.2166/nh.2016.110.

Marhaento, H., M. J. Booij, and A. Y. Hoekstra. 2018. "Hydrological response to future land-use change and climate change in a tropical catchment." *Hydrol. Sci. J.* 63 (9): 1368–1385. https://doi.org/10.1080/02626667.2018.1511054.

Marhaento, H., M. J. Booij, T. H. M. Rientjes, and A. Y. Hoekstra. 2017b. "Attribution of changes in the water balance of a tropical catchment to land use change using the SWAT model." *Hydrol. Processes* 31 (11): 2029–2040. https://doi.org/10.1002/hyp.11167.

McGarigal, K., S. A. Cushman, and E. Ene. 2012. "FRAGSTATS: Spatial pattern analysis program for categorical maps." Univ. of Massachusetts, Amherst. Accessed March 22, 2018. http://www.umass.edu/landeco/research/fragstats/fragstats.html.

McGarigal, K., and B. J. Marks. 1995. *FRAGSTATS: Spatial pattern analysis program for quantifying landscape structure*. General Technical Rep. No. PNW-GTR-351. Portland, OR: USDA, Forest Service, Pacific Northwest Research Station.

Mejía, A. I., and G. E. Moglen. 2009. "Spatial patterns of urban development from optimization of flood peaks and imperviousness-based measures." *J. Hydrol. Eng.* 14 (4): 416–424. https://doi.org/10.1061/(ASCE)1084-0699(2009)14:4(416).

Memarian, H., S. K. Balasundram, K. C. Abbaspour, J. B. Talib, C. T. Boon Sung, and A. M. Sood. 2014. "SWAT-based hydrological modelling of tropical land-use scenarios." *Hydrol. Sci. J.* 59 (10): 1808–1829. https://doi.org/10.1080/02626667.2014.892598.

Neitsch, S. L., J. G. Arnold, J. R. Kiniry, and J. R. Williams. 2011. *Soil and water assessment tool theoretical documentation version 2009*. College Station, TX: Texas Water Resources Institute.

O'Connell, P. E., J. Ewen, G. O'Donnell, and P. Quinn. 2007. "Is there a link between agricultural land-use management and flooding?" *Hydrol. Earth Syst. Sci.* 11 (1): 96–107. https://doi.org/10.5194/hess-11-96-2007.

Remondi, F., P. Burlando, and D. Vollmer. 2016. "Exploring the hydrological impact of increasing urbanisation on a tropical river catchment of the metropolitan Jakarta, Indonesia." *Sustainable Cities Soc.* 20 (Jan): 210–221. https://doi.org/10.1016/j.scs.2015.10.001.

Roberts, A. D. 2016. "The effects of current landscape configuration on streamflow within selected small watersheds of the Atlanta metropolitan region." *J. Hydrol. Reg. Stud.* 5 (Mar): 276–292. https://doi.org/10.1016/j.ejrh.2015.11.002.

Romanowicz, R. J., and M. J. Booij. 2011. "Impact of land use and water management on hydrological processes under varying climatic conditions." *Phys. Chem. Earth, Parts A/B/C* 36 (13): 613–614. https://doi.org/10.1016/j.pce.2011.08.009.

Sahin, V., and M. J. Hall. 1996. "The effects of afforestation and deforestation on water yields." *J. Hydrol.* 178 (1–4): 293–309. https://doi.org/10.1016/0022-1694(95)02825-0.

Su, W., G. Ye, S. Yao, and G. Yang. 2014. "Urban land pattern impacts on floods in a new district of China." *Sustainability* 6 (10): 6488–6508. https://doi.org/10.3390/su6106488.

Suryatmojo, H., F. Masamitsu, K. Kosugi, and T. Mizuyama. 2011. "Impact of selective logging and intensive line planting system on runoff and soil erosion in a tropical Indonesia rainforest." In Vol. 46 of *Proc., River Basin Management VI*, 288–300. Southampton, UK: WIT Press.

Tague, C. L., and L. E. Band. 2004. "RHESSys: Regional hydro-ecologic simulation system—An object-oriented approach to spatially distributed modeling of carbon, water, and nutrient cycling." *Earth Interact.* 8 (19): 1–42. https://doi.org/10.1175/1087-3562(2004)8<1:RRHSSO>2.0.CO;2.

USGS. 2017. "LANDSAT products courtesy of the U.S. Geological Survey." Accessed July 9, 2017. https://earthexplorer.usgs.gov/.

Valentin, C., et al. 2008. "Runoff and sediment losses from 27 upland catchments in Southeast Asia: Impact of rapid land use changes and conservation practices." *Agric. Ecosyst. Environ.* 128 (4): 225–238. https://doi.org/10.1016/j.agee.2008.06.004.

Verburg, P. H., and J. Bouma. 1999. "Land use change under conditions of high population pressure: The case of Java." *Global Environ. Change* 9 (4): 303–312. https://doi.org/10.1016/S0959-3780(99)00175-2.

Wagner, P. D., S. Kumar, and K. Schneider. 2013. "An assessment of land use change impacts on the water resources of the Mula and Mutha Rivers catchment upstream of Pune, India." *Hydrol. Earth Syst. Sci.* 17 (6): 2233–2246. https://doi.org/10.5194/hess-17-2233-2013.

Wheater, H., and E. Evans. 2009. "Land use, water management and future flood risk." Supplement, *Land Use Policy* 26 (S1): S251–S264. https://doi.org/10.1016/j.landusepol.2009.08.019.

Wigmosta, M. S., and S. J. Burges. 1990. "Proposed model for evaluating urban hydrologic change." *J. Water Resour. Plann. Manage.* 116 (6): 742–763. https://doi.org/10.1061/(ASCE)0733-9496(1990)116:6(742).

Wilk, J., and D. A. Hughes. 2002. "Simulating the impacts of land-use and climate change on water resource availability for a large south Indian catchment." *Hydrol. Sci. J.* 47 (1): 19–30. https://doi.org/10.1080/02626660209492904.

Zhang, G., S. Guhathakurta, G. Dai, L. Wu, and L. Yan. 2013. "The control of land-use patterns for stormwater management at multiple spatial scales." *Environ. Manage.* 51 (3): 555–570. https://doi.org/10.1007/s00267-012-0004-6.

Zhang, L., Z. Nan, Y. Xu, and S. Li. 2016. "Hydrological impacts of land use change and climate variability in the headwater region of the Heihe River Basin, Northwest China." *PLoS One* 11 (6): e0158394. https://doi.org/10.1371/journal.pone.0158394.

J. Water Resour. Plann. Manage., 2019, 145(12): 04019054